RAPID COMMUNICATIONS

PHYSICAL REVIEW B VOLUME 48, NUMBER 14 1 OCTOBER 1993-II

Anisotropic transport properties of in-plane-aligned *a*-axis $YBa_2Cu_3O_7$ films

Y. Suzuki, D. Lew, A. F. Marshall, M. R. Beasley, and T. H. Geballe

Department of Applied Physics and Center for Materials Research, Stanford University, Stanford, California 94305

(Received 9 June 1993)

We have grown *a*-axis $YBa_2Cu_3O_7$ films aligned in the plane of the substrate (100) $LaSrGaO_4$ by off-axis sputtering. X-ray and TEM analysis show a single predominant orientation of the *b* and *c* axes in these films. In-plane texture x-ray scans and Rutherford backscattering spectroscopy channeling reveal good crystalline quality. TEM analysis shows antiphase boundaries in the [010] direction and stacking fault boundaries in the [001] direction. We obtain an anisotropy ratio in resistivity of 8. The anisotropy in resistivity as well as in critical current density is less than that in single crystals. The reduction can be accounted for by the small percentage of misoriented grains in these films. We also investigate the resistive properties of antiphase boundaries and stacking fault boundaries. The field dependence of the critical current density in the [010] and [001] directions is similar to that of *c*-axis films, which is known not to be weak link limited.

There has been much interest in the growth of $YBa_2Cu_3O_7$ (YBCO) films with the *a*-axis normal to the substrate for making sandwich-type Josephson junctions. These structures take advantage of the longer *a*-axis coherence length in contrast to the shorter *c*-axis coherence length. Akoh *et al.* and Lee *et al.* have shown an anisotropic proximity effect of YBCO in proximity effect junctions.[1] Barner *et al.*, Hashimoto *et al.*, and Lew *et al.* have grown *a*-axis YBCO/PBCO/YBCO junctions exhibiting Josephson coupling across *a*-axis $PrBa_2Cu_3O_7$ (PBCO).[2–4] Many groups have successfully fabricated *a*-axis oriented films on $SrTiO_3$, $LaAlO_3$, and $SrTiO_3$ buffered MgO among others by pulsed laser deposition and rf magnetron sputtering.[4–7] When *a*-axis films are grown on these cubic substrates, two types of domains nucleate, resulting in 90° grain boundaries as well as antiphase boundaries (APB). Electrical transport is a combination of a zig-zag current path along the CuO planes, grain boundary resistance, and possibly some *c*-axis transport. The properties of the 90° grain boundaries which may have different boundary planes varies as analyzed in these films and in (103) films. It has been shown that some grain boundaries, for example a 90° twist boundary, do not noticeably degrade the transport properties; the 90° twist boundary has been isolated in (103) films along the [010] direction and does not exhibit weak link behavior.[8] Others have yet to be isolated. In any event it is clear experimentally that some boundaries reduce the critical current density in the plane of traditional *a*-axis films and hence render them not ideal as electrodes of sandwich-type Josephson junctions. The critical current of the film is often less than that of the junction.

To reduce the effect of grain boundaries in *a*-axis films, several groups have grown *a*-axis films with the *c*-axes aligned in the plane of the substrate,[9,10] as well as (110) films with the c-axis aligned in the plane of the substrate.[11] The approach has been to choose a substrate whose surface unit cell is rectangular so that the *b* and *c* axes of YBCO preferentially align across the entire substrate. Hontsu *et al.* have grown successfully *a*-axis YBCO films buffered with PBCO on $LaSrGaO_4$ (LSGO) substrates by pulsed laser deposition.[10] (100) LSGO has a rectangular unit cell of $b=3.843$ Å and $c=12.681$ Å. At the growth temperature the *b* axis of the LSGO matches the *b* axis of the PBCO very well, although there is a greater degree of mismatch for the *c* axis. X-ray-diffraction analysis shows that the *b* axis of the PBCO preferentially aligns with the *b* axis of LSGO. The subsequent YBCO layer grows epitaxially on the PBCO.

We have grown *a*-axis YBCO films aligned in the plane of the substrate using this buffering technique in a single target 90° off-axis sputtering system.[12] The growth pressure is maintained at 90 mtorr (60% Ar and 40% O_2). A buffer layer of PBCO is grown at 640 °C and a subsequent layer of YBCO is grown at 700 °C. The samples are oxygenated immediately after depositon as the samples cool to room temperature. The (100) LSGO substrates, supplied by Komatsu Co. Ltd., have excellent crystalline order with ω rocking curve full width at half maximum of 0.007°. AFM imaging of the substrate after cleaning shows the peak-to-valley ratio to be 100 Å with a standard deviation of 10 Å.

X-ray, RBS, TEM, and SEM analysis reveal a consistent picture of the microstructures of these films. X-ray-diffraction analysis shows 99.9% *a*-axis orientation with only traces of *c*-axis grains. An ω scan of the (200) YBCO peak shows a mosaic spread $\Delta\omega=0.47°$. RBS channeling shows good crystalline quality with $\chi_{min}=4.9\%$. The in-plane alignment of the domains is verified by a ϕ scan of the (102) YBCO peak; this scan suggests that 3–4 % of the domains are misaligned, i.e., have CuO planes at 90° to the majority of CuO planes (Fig. 1). SEM images indicate an elongated growth structure with an average *b*-axis/*c*-axis aspect ratio of 3. A typical domain has a width of 300 Å and length of 1000 Å. AFM confirms this structure and shows a peak-to-valley ratio of 250±50 Å for the film.

A transmission electron microscope (TEM) image of a

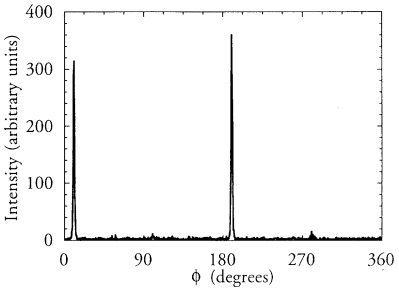

FIG. 1. In-plane texture x-ray scan of the (102) YBCO peak of an aligned *a*-axis film.

typical film is shown in planar view in Figs. 2(a) and 2(b). The majority of the material has a *b*-axis orientation aligned in one direction in the plane of the film as expected from x-ray analysis. Hence most of the 90° grain boundaries that are normally present in traditional *a*-axis films on cubic substrates are absent. However, a boundary structure is still observed indicating that during nucleation on the substrate, adjacent regions of the ordered 1:2:3 structure often nucleate out of registry with one another. This results in APB's along the [010] direction and in stacking faults (SF's) in the [001] direction. High-resolution TEM shows that an APB tends to terminate on a SF, so that relatively defect-free regions are enclosed by a combination of these planar defects. The material therefore has a kind of a "granular" structure. The connectivity of the boundaries indicates that most of the APB's and SF's are due to this nucleation effect rather than occurring as random defects in the film. These "grains" are elongated in the [010] direction, the nonordering direction, as indicated by SEM and AFM, with a width of 100 Å–500Å and a length of several hundred to several thousand Å. APB's with both a shift of $c/3$ and $c/6$ are observed. These APB's are being investigated in more detail in terms of the interface epitaxy and relative occurrence of the two types. It is interesting to note that for a $c/3$ shift one out of every two CuO planes connects with another such plane across the boundary. For a shift of $c/6$, none of the layers connect with a like layer. One might therefore expect different properties for these two types of APB's. Similarly several types of stacking faults are observed along the [001] direction, with stacking variations occurring both at the chain layer region of the unit cell and within. The TEM micrographs indicate that the density of misaligned domains is less than 2%, slightly lower than that inferred from ϕ scans. The 90° boundaries between an aligned region and a misaligned one are mostly faceted [100] tilt boundaries.

(a)

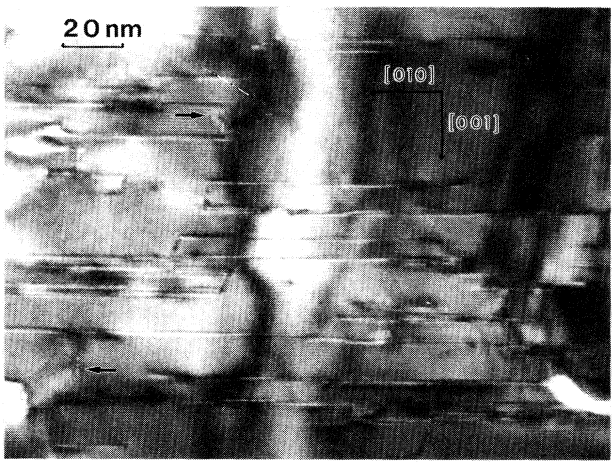

(b)

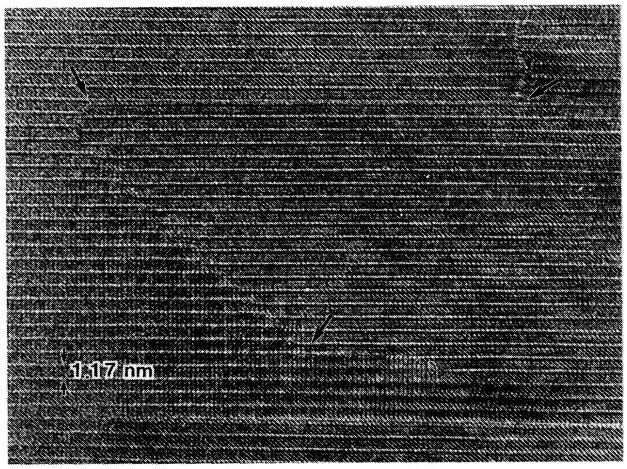

FIG. 2. (a) Low-resolution TEM plan view of an aligned *a*-axis film. The arrows indicate misaligned domains which are linked to the aligned domains mostly by 90° tilt boundaries. (b) High-resolution TEM plan view. The arrows indicate the inner section of antiphase boundaries (APB's) traversing the [010] direction and stacking faults (SF's) traversing the [001] direction.

Figure 3 shows the resistivity as a function of temperature in the [010] and [001] directions. The films have a sharp resistive transition at $T_{c0}=87$ K in both directions. In the [010] direction, the temperature dependence of resistivity exhibits metallic behavior; the slope of the normal state ($d\rho/dT$) is similar to that of a good *c*-axis film, which includes *b*-axis transport as well as *a*-axis transport and twin boundary resistance. We attribute the zero temperature intercept of the normal-state resistivity of 48$\mu\Omega$-cm to the APB's. The films also show metallic

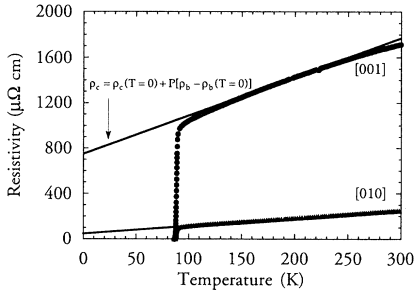

FIG. 3. Resistivity vs temperature in the [010] and [001] directions. The zero temperature intercept of the [010] resistivity yields a value for the resistance due to the APB's. The [001] resistivity is fit by the temperature dependence of the [010] resistivity which is primarily that along the CuO planes; however, current in the [001] direction flows perpendicular and parallel to the CuO planes in aligned and misaligned domains, respectively.

behavior in the normal state in the [001] direction. From single-crystal data we expect the resistivity in the [001] direction to be 30–100 times larger than that in the [010] direction.[13] The temperature dependence of the c-axis resistivity has not been unambiguously established. The anisotropy ratio in the aligned a-axis film is about 8 compared to the ratio of 2 obtained by Hontsu *et al.*[10] Since these films contain misaligned domains, we do not expect the anisotropy ratio to be as large as that of single crystals.

We can gain insight into the nature of the APB's and the boundaries between aligned and misaligned domains. We model the normal-state [010] transport as a parallel network of resistors representing intradomain resistances along the CuO planes linked together in series by resistors representing the APB resistances. Since the APB's contribute $R_{AP}=120\ \Omega$ or a resistivity of 48 $\mu\Omega$-cm as seen in Fig. 2, the resistance of a single APB is roughly $R_{ap}=(l_b/l_c)(L_c/L_b)R_{AP}=8\ \Omega$ where l_b and l_c are the average b- and c-axis dimensions of a domain and L_b and L_c are the macroscopic dimensions of the sample in the b and c directions; the sheet resistance is $R_{ap\square}=0.16\ \Omega/\square$. The conductance of an APB is $\sigma_{ap}=2.1\times10^{9}\ (\Omega\,\mathrm{cm}^2)^{-1}$. We believe that in the [010] direction the APB's are not shorted by a current path that goes around the APB by crossing a stacking fault in the [001] direction into the neighboring grain, traveling along the CuO planes and crossing back through a stacking fault in the [00$\bar{1}$] direction. Even assuming that the stacking fault contributes no resistance, we estimate the resistance thorough such a current path that shorts the APB's to be an order of magnitude larger than that of a single APB, R_{ap}. Therefore in the [010] direction the normal current flows along the CuO planes and through the APB's.

Normal-state transport in the [001] direction is greatly affected by misaligned domains, as is evident from the anisotropy and temperature dependence of the [001] conductivity. Along the [001] direction there are SF's between adjacent aligned domains while the boundaries between an aligned and misaligned domain are mostly 90° tilt boundaries. The [001] resistivity can be fit reasonably by the temperature dependence of the [010] resistivity, $\rho_c(T)=\rho_c(T=0)+P[\rho_b(T)-\rho_b(T=0)]$, where $P=5$ is the product of the mean percolative lengthening and mean shrinkage of current cross section (Fig. 3).[13] This suggests that the current flows essentially along the CuO planes. We can estimate the resistance for the limiting case that all the current flows along the CuO planes, i.e., SF's are boundaries of infinite resistance ($R_{sf}\rightarrow\infty$) and the 90° tilt boundaries contribute no resistance ($R_{tilt}=0$). We can model the transport current in the [001] direction to be flowing along the CuO planes in an aligned domain until it reaches a misaligned domain where it flows along the CuO planes in the macroscopic [001] direction. We assume a typical domain size of $1_b\times1_c=1000\ \text{Å}\times300\ \text{Å}$. Assuming that 4% of the domains are misaligned as seen in ϕ scans, we estimate the minimum resistance in the [001] direction to be more than an order of magnitude greater than the measured resistance. Therefore the temperature dependence of the measured [001] resistance cannot be attributed entirely to the CuO planes. Let us

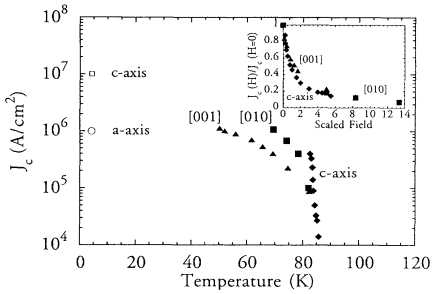

FIG. 4. J_c vs temperature in the [010] and [001] directions. The inset shows field dependence of the critical current density in the two directions at 77 K similar to that of a high-J_c c-axis film which is known to not be weak link limited. The scaled field is in kG for the c-axis film and in kG/$\sqrt{\text{mass ratio}}$ for the [010] and [001] directions of the aligned film.

assume that the macroscopic current in the [001] direction flows perpendicular to the CuO planes in aligned domains and along the CuO planes in the misaligned domains, i.e., R_{sf} and R_{tilt} are finite. We model the macroscopic current in the [001] direction as flowing through a network of misaligned and aligned domains that are linked in parallel and series by SF's and 90° tilt boundaries. For values of R_{sf} and $R_{tilt}\sim2\ \Omega$, which are not unreasonable, the experimental and theoretical values agree to within 20% in the normal state. This agreement indicates that the normal current flows perpendicular to the CuO planes as well as along the CuO planes.

Now we turn to the superconducting state. Critical current density (J_c) versus temperature of these aligned films are compared to that of c-axis films and traditional a-axis films (Fig. 4). The measured J_c in the [001] direction is lower than that of the highest J_c c-axis films as seen in Fig. 4. Since an upper estimate of J_c due to an APB ($J_c\sim\Delta\sigma_{ap}\sim10^7$ A/cm^2) is larger than that measured in the [010] direction, J_c[010] is not necessarily limited by the APB's. There may be more cation disorder in c-axis than a-axis films because while Y, Ba, and Cu arrive simultaneously during single-target sputtering at the film surface, in a c-axis film there is one cation species per layer whereas in an a-axis film *all* cation species are found in a given layer; such cation disorder in-

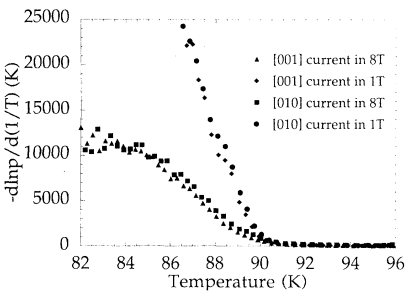

FIG. 5. Activation energy vs temperature when the current flows in the [010] and [001] directions and the field is applied perpendicular to the substrate.

creases pinning in c-axis films and thus increases J_c. Thus J_c [010] may be limited by intragrain pinning. Supercurrent in the [010] direction exhibits a field dependence similar to that of a high-J_c c-axis film which is known not to be weak link limited (Fig. 4 inset), further supporting the conclusion that J_c [010] is not limited by APB's.

The situation for J_c [001] is more complicated. J_c [001] falls below J_c [010] and is on the order of J_c of traditional a-axis films (see open symbols at low temperatures in Fig. 4). J_c [001] is a combination of misaligned and aligned domains if our estimate that R_{ap}, R_{sf}, and R_{tilt} are all of the same order of magnitude is accurate. J_c [001] also exhibits a field dependence similar to that in a high-J_c c-axis film. Given our conclusion that normal current flows at least to some degree in the [001] direction in our films, we conclude that in traditional a-axis films a similar situation may prevail.

To obtain a measure of pinning centers, we investigate resistive transitions in magnetic field in these aligned films. The current is applied in the [010] and [001] directions and the field is applied perpendicular to the substrate. The activation energy, as deduced from the slope of $\ln\rho$ versus $1/T$, is strongly temperature dependent in both current directions, as expected near T_{c0}. If the pinning were dominated by the CuO planes sandwiched by weakly superconducting regions, we would expect an anisotropy in the activation energies of the two directions. We see no such anisotropy (Fig. 5). This lack of anisotropy suggests that J_c [001] is not limited by supercurrent flowing perpendicular to the CuO planes.

In conclusion we have fabricated and characterized in-plane-aligned a-axis YBCO films on LSGO substrates. They show good alignment of the b and c axes as seen from x-ray and TEM analysis and good crystallinity from ϕ scans and RBS channeling. The alignment of domains in these films minimizes 90° grain boundary resistances and problems of low critical current densities found in traditional a-axis films. Due to a small amount of misaligned domains, the anisotropy in resistivity and critical current densities along the [010] and [001] directions is reduced from that seen in single crystals. We have been able to isolate APB's. Current in the [010] direction flows principally along the CuO planes and through the APB's. From the resistivity and J_c values, current in the [001] direction seems to flow perpendicular to the CuO planes in aligned domains and parallel to the CuO planes in misaligned domains; the temperature dependence of the [001] resistivity and the pinning energies suggest a current path following the CuO planes. These conclusions suggest a complicated current path in the [001] direction in the normal and superconducting states and the need for further investigation.

Note added in proof. Similar work has been published recently by M. Mukaida and S. Miyazawa, Appl. Phys. Lett. **63**, 999 (1993).

We thank K. B. Do for AFM imaging, C. B. Eom for RBS analysis and helpful discussions, T. Kawai for informing us of Ref. 10 and for assisting us in making contact with Komatsu Co. Ltd. whom we thank for supplying the LSGO substrates. This work was supported by Air Force Office of Scientific Research and the Electrical Power Research Institute. Y.S. acknowledges partial financial support from NSF.

[1]H. Akoh, C. Camerlingo, and S. Takeda, Appl. Phys. Lett. **56**, 1487 (1990); Mark Lee, D. Lew, C. B. Eom, T. H. Geballe, and M. R. Beasley, Appl. Phys. Lett. **57**, 1152 (1990).

[2]J. B. Barner, C. T. Rogers, A. Inam, R. Ramesh, and S. Bersey, Appl. Phys. Lett. **59**, 742 (1991).

[3]T. Hashimoto, M. Sagoi, Y. Mizutani, J. Yoshida, and K. Mizushima, Appl. Phys. Lett. **60**, 1756 (1992).

[4]D. Lew, Y. Suzuki, C. B. Eom, M. Lee, J.-M. Triscone, T. H. Geballe, and M. R. Beasley, Physica C **185-189**, 2553 (1991).

[5]C. B. Eom, A. F. Marshall, S. S. Laderman, R. D. Jacowitz, and T. H. Geballe, Science **249**, 1549 (1990).

[6]K. Char, M. R. Hahn, T. L. Hylton, M. R. Beasley, T. H. Geballe, and A. Kapitulnik, IEEE Trans. Magn. **25**, 2422 (1989).

[7]A. Inam, C. T. Rogers, R. Ramesh, L. Farrow, K. Remschnig, D. Hart, and T. Venkatesan, Appl. Phys. Lett **57**, 2484 (1990).

[8]C. B. Eom, A. F. Marshall, Y. Suzuki, B. Boyer, R. F. W. Pease, and T. H. Geballe, Nature (London) **353**, 544 (1991); C. B. Eom, A. F. Marshall, Y. Suzuki, T. H. Geballe, B. Boyer, R. F. W. Pease, R. B. van Dover, and J. M. Phillips, Phys. Rev. B **46**, 11 902 (1992).

[9]K. H. Young and J. Z. Sun, Appl. Phys. Lett. **59**, 2448 (1991).

[10]S. Hontsu, J. Ishii, T. Kawai, and S. Kawai, Appl. Phys. Lett. **59**, 2886 (1991); S. Hontsu, N. Mukai, J. Ishii, T. Kawai, and S. Kawai, Appl. Phys. Lett. **61**, 1134 (1992).

[11]J. Z. Wu, P. Y. Hsieh, A. V. McGuire, D. L. Schmidt, L. T. Wood, Y. Shen, and W. K. Chu, Phys. Rev. B **44**, 12 643 (1991).

[12]C. B. Eom, J. Z. Sun, K. Yamamoto, A. F. Marshall, K. E. Luther, T. H. Geballe, and S. S. Laderman, Appl. Phys. Lett. **55**, 595 (1989).

[13]Y. Iye, T. Tamegai, T. Sakakibara, T. Goto, N. Miura, H. Takeya, and H. Takei, Physica C **153-155**, 26 (1988); S. W. Tozer, A. W. Kleinasser, T. Penney, D. Kaiser, and F. Holtzberg, Phys. Rev. Lett. **59**, 1768 (1987); T. K. Worthington, W. J. Gallagher, D. L. Kaiser, F. H. Holtzberg, and T. R. Dinger, Physica C **153-155**, 32 (1988).

[14]J. Halbritter, Int. J. Mod. Phys. **3**, 719 (1989).

(a)

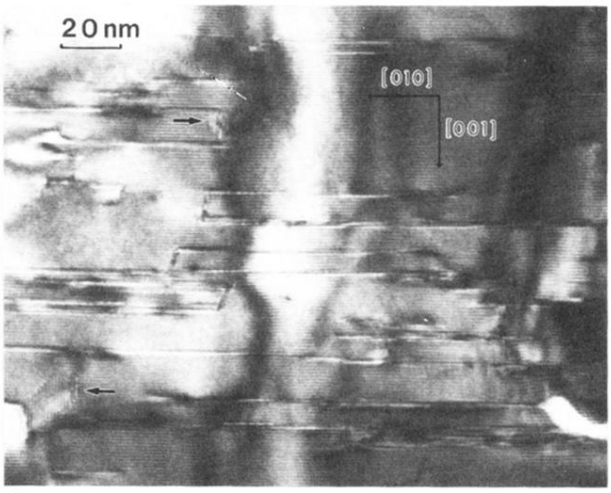

(b)

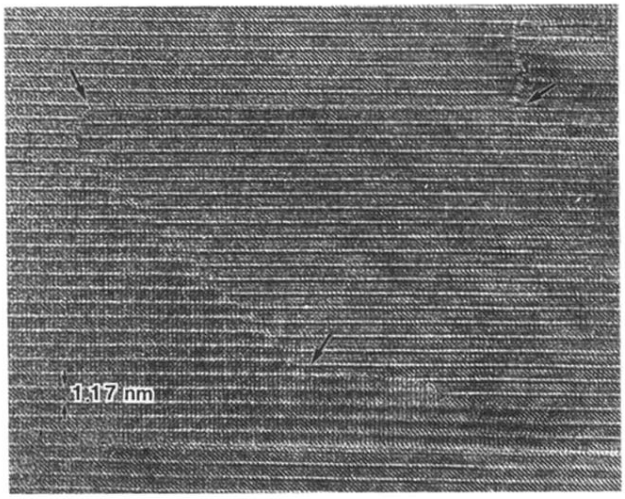

FIG. 2. (a) Low-resolution TEM plan view of an aligned *a*-axis film. The arrows indicate misaligned domains which are linked to the aligned domains mostly by 90° tilt boundaries. (b) High-resolution TEM plan view. The arrows indicate the inner section of antiphase boundaries (APB's) traversing the [010] direction and stacking faults (SF's) traversing the [001] direction.